INTERNATIONAL JOURNAL FOR NUMERICAL METHODS IN FLUIDS
Int. J. Numer. Meth. Fluids 2001; **36**: 925–945 (DOI: 10.1002/fld.157)

An implicit time-marching algorithm for shallow water models based on the generalized wave continuity equation

Kendra M. Dresback*,[1] and Randall L. Kolar

School of Civil Engineering and Environmental Science, University of Oklahoma, Norman, OK, U.S.A.

SUMMARY

Wave equation models currently discretize the generalized wave continuity equation with a three-time-level scheme centered at k and the momentum equation with a two-time-level scheme centered at $k+1/2$; non-linear terms are evaluated explicitly. However in highly non-linear applications, the algorithm becomes unstable at even moderate Courant numbers. This paper examines an implicit treatment of the non-linear terms using an iterative time-marching algorithm. Depending on the domain, results from one-dimensional experiments show up to a tenfold increase in stability and temporal accuracy. The sensitivity of stability to variations in the G-parameter (a numerical weighting parameter in the generalized wave continuity equation) was examined; results show that the greatest increase in stability occurs with $G/\tau = 2-50$. In the one-dimensional experiments, three different types of node spacing techniques—constant, variable, and LTEA (Localized Truncation Error Analysis)—were examined; stability is positively correlated to the uniformity of the node spacing. Lastly, a scaling analysis demonstrates that the magnitudes of the non-linear terms are positively correlated to those that most influence stability, particularly the term containing the G-parameter. It is evident that the new algorithm improves stability and temporal accuracy in a cost-effective manner. Copyright © 2001 John Wiley & Sons, Ltd.

KEY WORDS: finite elements; generalized wave continuity; implicit time-marching; shallow water equations

1. INTRODUCTION

Shallow water equations are based on the depth-averaged equations of motion, subject to the assumption of a hydrostatic pressure distribution; they are used by researchers and engineers

* Correspondence to: School of Civil Engineering and Environmental Science, University of Oklahoma, 202 West Boyd Street, Room 334, Norman, OK 73019-1024, U.S.A. Tel.: +1 405 3255218; fax: +1 405 3254217.
[1] E-mail: dresback@ou.edu

Received 11 October 1999
Accepted 19 September 2000

to model the hydrodynamic behavior of oceans, coastal areas, estuaries, lakes and impoundments [1]. Early finite element solutions of the primitive shallow water equations were plagued with spurious oscillations. Lynch and Gray [2] in 1979 introduced the wave continuity equation (WCE), which suppressed the spurious oscillations without having to dampen the solution either numerically or artificially. Kinnmark [3] determined that there was no loss in the wave propagation characteristics of the wave continuity equation if, during the formulation, the bottom friction τ is replaced by a numerical parameter G, thus developing the generalized wave continuity equation (GWCE). With this G-parameter, it is possible to achieve a balance between the primitive form and pure wave form of the shallow water equations. Several models have been developed from the GWCE and the WCE since their inception 20 years ago, including the model used in this paper, ADCIRC (an ADvanced three-dimensional CIRCulation model) [4,5].

With ADCIRC, non-linear applications have stability problems unless a severe Courant number restriction is imposed. In practice, we have found that a practical upper bound of the Courant number is 0.5 in order to maintain the stability of the model; an even tighter constraint must be imposed if the simulation includes barrier islands and constricted inlets. In order to relax this restriction, an alternative time-marching procedure was proposed that treats some or all of the non-linear terms implicitly [6].

In the early years of finite element shallow water models, a number of studies looked at time-marching, but often from a noise suppression point-of-view. For example, Lee and Froehlich [7] summarize several time-marching procedures in their review paper on shallow water equations, which covers everything from the trapezoidal rule to three-level semi-implicit schemes. Gray and Lynch [8] studied several of the same time-marching procedures in greater detail. In their paper, they indicate that the best scheme for finite element shallow water models is the three-level semi-implicit scheme. Several years later Kinnmark and Gray [9] examined a semi-implicit wave equation that produced accurate results, yet still treated some non-linear terms explicitly. Most of the more recent work with GWCE-based models has focused either on incorporating more physics or minimizing spatial error, e.g. alternative meshing criteria [10,11], wetting and drying [12], treatment of boundary conditions [13,14], three-dimensional baroclinic simulations [15,16], and more accurate estimates of the vertical velocity [17]. Furthermore, attempts to achieve timely simulations have led to parallel codes [18,19]. Little recent work with GWCE-based models has been devoted to alternative time-marching algorithms. The intent of this study is to fill this gap, viz., an implicit treatment of non-linear terms in both the GWCE and the momentum equation.

An implicit treatment can be realized by either simultaneous integration of the full non-linear equations or a predictor–corrector algorithm. A predictor–corrector algorithm was chosen over the simultaneous integration for the following reasons: (1) it can be easily implemented within the framework of the existing ADCIRC code; and (2) it minimizes the size of the matrices that must be stored and inverted. The primary goal of this article is to assess the impact of the predictor–corrector algorithm on the stability, accuracy, and the sensitivity of a one-dimensional version of the ADCIRC code.

2. SHALLOW WATER EQUATIONS

Many sources provide the full shallow water equations [2–5,10,20,21] so for purposes of brevity, only the GWCE and non-conservative form of the momentum (NCM) equation will be shown; they form the basis of the ADCIRC model. Below is the operator form of the GWCE, where L represents the primitive continuity equation, $\mathbf{M}^C$ is the conservative form of the momentum equation and G is a numerical parameter

$$W^G \equiv \frac{\partial L}{\partial t} + GL - \nabla \cdot \mathbf{M}^C \tag{1}$$

Lynch and Gray's [2] WCE can be obtained by setting $G = \tau$, where τ is the bottom friction coefficient. It should be noted that the higher the value of G, the more the GWCE approaches the primitive equation. Expanded versions of the GWCE and NCM equation are shown below and all terms are described in the nomenclature section; the predominant terms are explained below the equations. The abbreviations appearing above certain terms in these equations will be discussed in subsequent sections.

GWCE

$$W^G \equiv \frac{\partial^2 \zeta}{\partial t^2} + G\frac{\partial \zeta}{\partial t} + G\overset{\text{'Gg'}}{\nabla \cdot}(H\mathbf{v}) - \tau\overset{\text{'bg'}}{\nabla \cdot}(H\mathbf{v}) - \nabla \cdot \left\{ \overset{\text{'ag'}}{\nabla \cdot}(H\mathbf{v}\mathbf{v}) + H\mathbf{f} \times \mathbf{v} + H\nabla\left[\frac{p_a}{\rho} + g(\zeta - \overset{\text{'fg'}}{\alpha\eta})\right] - \mathbf{A} - \frac{1}{\rho}\nabla \cdot (H\mathbf{T}) \right\} - H\mathbf{v} \cdot \nabla\tau = 0 \tag{2}$$

NCM Equation

$$\mathbf{M} \equiv \frac{\partial \mathbf{v}}{\partial t} + \overset{\text{'am'}}{\mathbf{v} \cdot \nabla}\mathbf{v} + \tau\mathbf{v} + \mathbf{f} \times \mathbf{v} + \nabla\left[\frac{p_a}{\rho} + g(\zeta - \alpha\eta)\right] - \frac{\mathbf{A}}{H} - \frac{1}{\rho H}\nabla \cdot (H\mathbf{T}) = 0 \tag{3}$$

where ζ is the elevation of the water surface above the datum, t is time, G is the numerical parameter, $\mathbf{v}$ is the depth-averaged velocity of the fluid and H is the total fluid depth.

Algorithms based on these two equations result in solutions that compare well with analytical solutions and field data for both elevation and velocity. The codes typically use equal-order finite element interpolating functions (linear C^0 elements). As presently derived, semi-implicit time discretization of the GWCE uses a three-time-level approximation centered at k, while time discretization of the NCM equation uses a lumped two-time-level approximation centered at $k + 1/2$. Equations are linearized by formulating the non-linear terms explicitly. Exact quadrature rules are used. Product terms in the equations are simplified by linearly interpolating the products of the variables, not the individual variables. L_2 interpolation is applied to the advective terms in the equations. A time-splitting solution procedure is adopted wherein the GWCE is first solved for nodal elevations and then the NCM equation is solved for the velocity field. Resulting discrete equations can be found in Luettich *et al.* [4]

3. CHANGES IN THE TIME-MARCHING ALGORITHM

As a point of departure, let us first look in more detail at the current time-marching algorithm used in the ADCIRC model. As mentioned, it is a semi-implicit evaluation, i.e., the linear terms of the equation are evaluated implicitly and the non-linear terms of the equation are evaluated explicitly. At the past and present time levels in ADCIRC, elevation and velocity values are known (either from initial conditions or previous calculations). The original algorithm takes the elevation and velocity values for the past $(k-1)$ and the present (k) and uses them to calculate the values for the future $(k+1)$ time level. However, the non-linear terms are evaluated using only the elevation and velocity values at the present time level (k). Kolar *et al.* [6] hypothesized that the stability constraint stems primarily from this explicit evaluation of non-linear terms.

In order to evaluate the non-linear terms implicitly, a predictor–corrector algorithm is introduced. Two stages are most commonly used in a predictor–corrector algorithm. In this case the predictor stage is equivalent to the original algorithm, i.e. it evaluates the non-linear terms using values from the present. Predicted future values obtained from the predictor step (called k^*) and the already known present (k) and past $(k-1)$ values are then used to obtain the corrected values for the future time level $(k+1)$. The corrector stage can be repeated as many times as necessary until convergence. However, if multiple iterations are required, this iterative strategy will no longer be the most cost effective method of solution and a new form of linearization would be sought.

Non-linear terms exist in both governing equations for ADCIRC—the NCM and GWCE. Our study focuses on five dominant non-linear terms that are identified in Equations (2) and (3). Four are from the GWCE: advective (ag), finite amplitude (fg), GWCE flux times G (Gg) and GWCE flux times τ (bg) and one is from the NCM equation, the advective term (am). Table I summarizes the nomenclature for the non-linear terms in the governing equations.

Another issue with the predictor–corrector algorithm is the 'best' choice of time-weighting factors for the non-linear terms. Time weights multiply the non-linear terms that are evaluated at different levels. Note that time-weighting factors are only used in the corrector step of the new algorithm because the predictor step is evaluated explicitly. Time weights are noted in the equations by the abbreviations described above; the numbers that follow these abbreviations represent the time levels (1, time level $k+1$ or k^*; 2, time level k; 3, time level $k-1$). Pseudo code for the predictor–corrector algorithm for two of the non-linear terms is shown in Figure 1. The first box contains the predictor step for each of the non-linear terms; it uses no time

Table I. Nomenclature for non-linear terms.

Abbreviation	Term	Description
ag	$\nabla \cdot H\mathbf{vv}$	GWCE advective
fg	$\nabla \cdot Hg\nabla\zeta$	GWCE finite amplitude
Gg	$G\nabla \cdot (H\mathbf{v})$	GWCE flux times G
bg	$\tau\nabla \cdot (H\mathbf{v})$	GWCE flux times τ
am	$\mathbf{v} \cdot \nabla\mathbf{v}$	NCM advective

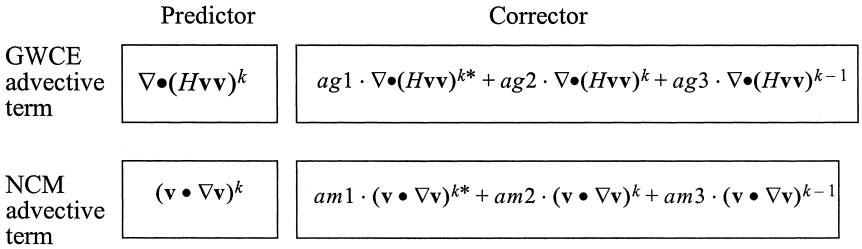

Figure 1. Predictor–corrector equations (examples) for two non-linear terms—the GWCE and NCM advective terms.

weights and provides the estimate of the elevation and velocity values at the future time level (k*). The second box contains the corrector step for each of the non-linear terms; it shows how the time weights multiply the non-linear terms at each time level. In the first corrector box of Figure 1, we see ag1, ag2 and ag3, are the time weights for the $k+1$ (or k*), k, $k-1$ time levels (future, present and past), respectively, for the advective term of the GWCE. Each non-linear term follows the same representation. In theory, the time-weighting parameters for the non-linear terms may equal any value as long as they sum to one; for practical reasons, the values are restricted to lie between zero and one.

Table II illustrates some possible choices for the time weights. For this paper, 'centered at k' (example 1 in Table II) means that the time weights for the non-linear terms are weighted equally between the three time levels; 'centered at $k+1/2$' (example 2 in Table II) means that the terms are weighted equally between the first two time levels; 'turned off' (example 5 in Table II) means that it is being evaluated explicitly, i.e. the original time-marching algorithm. Exhaustive studies will be conducted on how the variation of these time-weighting parameters affect the stability and accuracy of the code.

Table II. Possible combinations of the time-weighting parameters for the ag non-linear term.

Example number	ag1 (k* or $k+1$)	ag2 (k)	ag3 ($k-1$)	Sum
1	0.33	0.34	0.33	1.0
2	0.5	0.5	0.0	1.0
3	0.6	0.2	0.2	1.0
4	0.8	0.2	0.0	1.0
5	0.0	1.0	0.0	1.0

4. DOMAINS EVALUATED

One-dimensional studies using five different domains were conducted to determine if the predictor–corrector algorithm improved the stability of ADCIRC. Common conditions used in each of the domains are as follows: one-dimensional flow, constant bottom friction coefficient of 10^{-4} s^{-1}, a G/τ ratio of 10 (constant unless noted otherwise) and eddy visocity of 0. For each domain, the boundary conditions were as follows: forcing with a 1 m M_2 tide at the ocean boundary and no normal flux at the land boundary. The five domains evaluated were: constant bathymetry (Figure 2(a)), three parabolic bathymetries with varying rates of rise (Figure 2(b)) and the western North Atlantic bathymetry (east coast, Figure 2(c)). Maximum and minimum depths for the parabolic bathymetries were 300 and 3 m, respectively, while for the east coast bathymetry the values were 5000 and 20 m, respectively.

The constant bathymetry problem was evaluated using a constant spatial discretization with Δx based on a wavelength to node spacing ratio[2] of 200 for the M_2 tide, thus minimizing spatial truncation errors. The three bathymetries—second-order, fourth-order and fifth-order[3]—used two spatial discretizations, constant and variable. For the constant spatial

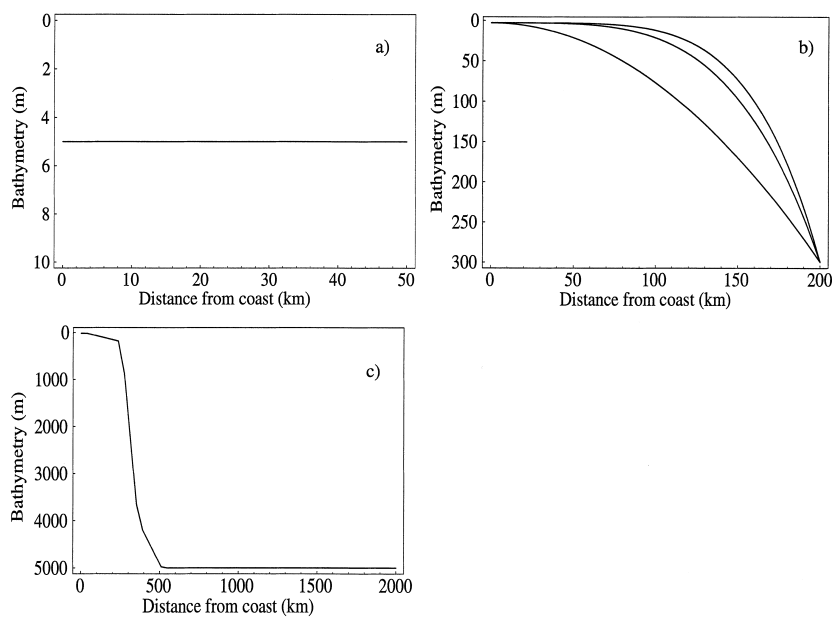

Figure 2. Schematics of the one-dimensional bathymetries: (a) constant, (b) quadratic-like, (c) east coast.

[2] Abbreviated $\lambda/\Delta x$, where $\lambda = \sqrt{gh} \times T$ and ?x is the distance between each node. In applications, the $\lambda/\Delta x$ ratio is recommended to be greater than 25.

[3] Order of the bathymetry refers to the order of polynomial used to generate the bathymetry data.

discretization, the wavelength was determined using the shallowest bathymetry of the domain and the time period for an M_2 tidal constituent. Using a $\lambda/\Delta x$ of 200, a Δx value was then determined and used throughout the domain. Thus, deeper portions of the domain were even more finely resolved. Non-uniform spatial discretization was developed using a $\lambda/\Delta x$ value of 300. Node placement for these grids are based on the bathymetry values at the current element location, meaning that Δx changes with the bathymetry. Spatial discretizations for the east coast bathymetry include the constant and two non-uniform techniques, $\lambda/\Delta x$ of 300 and the LTEA (Localized Truncation Error Analysis) method. In the latter, which was developed by Hagen [22], nodes are placed to minimize spatial truncation error.

Experiments conducted on the five bathymetries looked at the following: stability, which includes looking at the impact of the non-linear terms, individually and together; the number of corrector steps that are needed to obtain convergence and the maximum gains in stability; sensitivity to the G/τ ratio; and temporal accuracy. A scaling analysis was also performed to determine if there was a correlation between the magnitude of the terms and the results from the stability experiments. All tests are summarized in the experimental matrix given in Table III. Note that for the last three experiments, we chose the second-order bathymetry to be representative of the parabolic family.

5. NUMERICAL EXPERIMENTS AND DISCUSSION

5.1. Defining stability for non-linear simulations

Traditional stability studies, such as Fourier analysis, are valid for linear problems. Here, the non-linear terms preclude the use of such analytical methods, thus numerical experiments were used to determine stability. For each simulation, the maximum stable time step, to the nearest 5 s, was defined as that which can be used without causing overflow errors before the end of

Table III. Experimental matrix ($\times$ indicates experiments performed).

Domains[a]	Iteration analysis	Stability—individual	Stability—all terms	G sensitivity analysis	Temporal accuracy analysis	Scaling analysis
Constant	$\times$	$\times$	$\times$	$\times$	$\times$	$\times$
2C	$\times$	$\times$	$\times$	$\times$	$\times$	$\times$
2V		$\times$	$\times$			
4C	$\times$	$\times$	$\times$			
4V		$\times$	$\times$			
5C		$\times$	$\times$			
5V		$\times$	$\times$			
ECC	$\times$	$\times$	$\times$	$\times$		$\times$
ECV		$\times$	$\times$			
ECL		$\times$	$\times$		$\times$	

[a] Prefixes: 2, second-order; 4, fourth-order; 5, fifth-order; EC, east coast; and suffixes: C, constant spatial discretization; V, $\lambda/\Delta x$ (variable) spatial discretization; L, LTEA spatial discretization.

the simulation. Stability changes with the predictor–corrector algorithm were determined from these steps: (1) each domain was evaluated using the original algorithm to obtain the maximum stable time step for each type of spatial discretization; (2) each domain was evaluated using the predictor–corrector algorithm to obtain the maximum stable time step for each type of spatial discretization; (3) results from the two previous steps were compared to one another, and a per cent change between the two resulting time steps was obtained. It should be noted that since each corrector iteration requires another solution to the system matrix, only simulations that show more than a $n \times 100$ per cent change, where n is the number of corrector steps, are considered cost-effective. This is a conservative estimate because it assumes the entire load vector is re-evaluated with each iteration, while in reality, only the $k^*/k+1$ portion of the non-linear terms needs to be updated.

5.2. Iteration experiments

We examined two different issues with regard to the number of corrector iterations. The first issue, which can be considered more of a stability issue, involved determining the number of corrector iterations needed before the value of maximum stable time step did not change. The second issue, which is more of an accuracy issue, was to evaluate whether additional corrector iterations were needed to reach convergence for the elevation and velocity fields.

To address the stability issue, we performed experiments using three different bathymetry types (constant, fourth-order and east coast) and determined that the maximum stable time step did not vary greatly (0–5 per cent) from one to three corrector iterations. However, one term, the GWCE flux times G term (Gg, see Equation (2)) when updated independently in the east coast domain, shows a non-trivial decrease in the maximum stable time step from the first corrector iteration to the second corrector iteration, after which it stabilized. Closer analysis of this problem shows that a neutrally stable situation is reached with one corrector iteration, i.e. the solution remains bounded, but the results are not physically realistic. When more than one corrector iteration was used, results with the smaller time step are realistic.

Regarding the accuracy issue, we performed experiments on three different bathymetries (constant, second-order and east coast) to determine the number of iterations needed for the solution to converge. An L_2 norm was used to measure the difference between the elevation and velocity solutions from successive corrector iterations. Results show that the average L_2 norm between the first and second corrector iteration was on the order of 10^{-5}–10^{-7} ft or ft s^{-1}, depending on the domain, when updating all non-linear terms together using the centered scheme since the magnitude of the solution was on the order of 10^{-1}–10^{1}, we considered this sufficiently converged.

A general conclusion from the stability-related iteration tests is that a single iteration of the corrector step is sufficient unless the GWCE flux times G term is the only non-linear term updated, in which case two corrector iterations are recommended. Accuracy-related results show that a single iteration is needed to reach convergence. Moreover, our experience shows that spatial truncation errors generally dominate temporal truncation errors. Thus, taken together, the evidence suggests a single corrector iteration is adequate and was used in the remainder of the experiments. This means that a per cent increase in Δt of 100 is the minimum needed for the algorithm to be cost-effective.

5.3. Stability testing—non-linear terms evaluated individually

For the numerical experiments with the predictor–corrector algorithm, each non-linear term was evaluated individually with the following time weights: (1) centered at k, e.g., the ag term would have the time weights of example 1 in Table II, while the fg, Gg, am, and bg terms would be 'turned off' as in example 5 in Table II; (2) centered at $k+1/2$, e.g., the ag term would have the time weights of example 2 in Table II, while the fg, Gg, am, and bg terms would be 'turned off' as in example 5 in Table II.

Results are summarized in Table IV where positive increases in the allowable time step are shown in bold. Recall that a 100 per cent change is required for the algorithm to be cost-effective. In short, the major findings from the stability experiments on individual terms are as follows: (1) with the predictor–corrector algorithm, more than 100 per cent change in the maximum stable time step can be realized for most of the domains by iterating on the GWCE flux times G term (Gg); some of the simulations displayed over a tenfold increase from the original algorithm, and it should be noted that in these cases the Courant number is greater than one; (2) for the non-linear terms in the GWCE, the 'centered at k' time-weighting scheme produced the greatest increase in the stability; (3) for all the domains evaluated, constant spatial discretization allows for a greater per cent increase in the maximum stable time step than the variable spatial discretization (this does not necessarily imply a higher Courant number); and (4) the largest decreases in stability were found when the non-linear terms used a time-weighting scheme that is different from the original equation's time-weighting scheme.

5.4. Stability tests—non-linear terms evaluated together

Next we evaluated whether an implicit treatment of more than one of the non-linear terms would provide greater changes in stability. For each domain, we systemically determined the combination of the non-linear terms that resulted in the largest maximum stable time step (see Table IV, the 'Opt.' column). Note that we also determined the maximum stable time step with the non-linear terms evaluated with time weights that matched the centered implicit treatment of the linear terms (see Table IV, the 'Center' column). As previously mentioned, for a single corrector iteration, the per cent change between the new and baseline Δt must be greater than 100 per cent in order to be cost effective.

Results indicate that for most of the domains, the largest increase in stability was realized when four of the non-linear terms were updated, viz., the finite amplitude term (fg), GWCE flux times G term (Gg), GWCE flux times τ term (bg), and the advective term of the NCM equation (am). An exception is the constant bathymetry case, which demonstrated the largest increase in the maximum stable time step with two non-linear terms (GWCE flux times G term (Gg) and the advective term of the NCM equation (am)) being updated. The east coast domain with constant spatial discretization provided the greatest per cent increase in the time step. With few exceptions, optimum results were realized when the GWCE non-linear terms were centered at k and the NCM non-linear term was centered at $k+1/2$, which follows the formulation of the other terms in the equations. An exception to this in every domain was the GWCE advective term (ag), which put all the weight on the present time level; also in the constant and parabolic-like bathymetries, the GWCE flux times G term (Gg) used a fully implicit time-weighting scheme. Results for the fully centered scheme indicate that there was a

Table IV. Stability results—per cent changes in allowable time step (Bold indicates positive changes).

Domains[a]	Time weights for individual terms										All terms implicit	
	Centered at k					Centered at $k+1/2$					Opt.[b]	Center[c]
	ag	fg	Gg	bg	am	ag	fg	Gg	bg	am		
Constant	0.0	−3.7	**59.3**	−3.7	**3.7**	−22.2	0.0	**55.6**	0.0	**18.5**	**232**	**133**
2C	0.0	0.0	**433**	0.0	0.0	0.0	0.0	**189**	0.0	0.0	**1678**	**767**
2V	0.0	**57.9**	0.0	0.0	0.0	0.0	−94.7	0.0	0.0	0.0	**489**	**432**
4C	0.0	0.0	**356**	0.0	0.0	0.0	−44.4	**200**	0.0	0.0	**822**	**456**
4V	**64.3**	**57.1**	**57.1**	0.0	0.0	**21.4**	−78.6	**85.7**	0.0	0.0	**386**	**200**
5C	0.0	0.0	**641**	−5.9	0.0	0.0	0.0	**165**	−5.9	0.0	**641**	**224**
5V	**9.1**	−4.5	**77.3**	−9.1	0.0	−36.4	−90.9	**72.7**	−9.1	0.0	**241**	**114**
ECC	0.0	0.0	**8480**	0.0	0.0	0.0	0.0	**160**	0.0	0.0	**9780**	**5100**
ECV	0.0	0.0	**1345**	−6.1	0.0	0.0	−12.1	**345**	−6.1	0.0	**1458**	**1458**
ECL	0.0	0.0	**3038**	−7.7	0.0	0.0	0.0	**169**	−7.7	0.0	**3915**	**1024**

[a] Where prefixes: 2, second-order; 4, fourth-order; 5, fifth-order; EC, east coast; and suffixes: C, constant spatial discretization; V, $\lambda/\Delta x$ (variable) spatial discretization; L, LTEA spatial discretization.
[b] Optimum set of parameters—considered all possible combinations of the non-linear terms and time weights.
[c] Centered scheme—all GWCE non-linear terms are centered at k and the NCM non-linear terms is centered at $k+1/2$.

decrease in the maximum stable time step as compared to the optimum; however, all results achieved the 100 per cent threshold.

The most notable observation, and the underlying premise of the paper, was that all domains and discretization types far exceeded the 100 per cent threshold when using a centered or optimum combination of the non-linear terms. Comparing this to the stability experiments with the non-linear terms analyzed individually, we found that in all but one domain (fifth-order bathymetry), the increase in stability was greater when updating several non-linear terms together rather than individually. It is significant that the Courant number for all of the results in this section is much greater than one (the upper-bound for the original semi-implicit code). In all cases, the variable spatial discretization showed the greatest increase in the Courant number for the shallow bathymetries, while the constant spatial discretization showed the greatest increase in the deeper bathymetries.

5.5. G sensitivity tests

Sensitivity studies provide information on how parameter changes affect the outcome of the solution. For this study, we wanted to determine the affect of G, the numerical parameter in the GWCE, on the maximum stable time step, particularly since this non-linear term impacts the stability of the one-dimensional problems the most. Sensitivity analyses were conducted on three domains, which represent a wide range of conditions: constant bathymetry with constant spatial discretization, second-order bathymetry with constant spatial discretization and the east coast bathymetry with LTEA spatial discretization. The G-parameter ranged from 0.00001 to 0.1 s^{-1}, while the bottom friction coefficient, τ, was kept constant at 0.0001 s^{-1}. Simulations used the predictor–corrector algorithm with all the GWCE non-linear terms centered at k and the NCM non-linear term centered at $k+1/2$. For each parameter value, the maximum stable time step was obtained, which was then compared to the maximum stable time step from the original algorithm with G held constant at 0.001 s^{-1}.[4] per centage changes between the two were then calculated; results are shown in Figure 3. From Figure 3(a), it is evident that for the constant bathymetry the greatest per cent increase in stability occurs when the G/τ ratio is between 2 and 50 with the peak just past 30. Figure 3(b) shows that for the second-order bathymetry the greatest per cent increase in stability occurs with a G/τ ratio between 2 and 50 with the peak just past 10, while in Figure 3(c), we see that for the east coast bathymetry the greatest per cent increase occurs when the G/τ ratio is between 5 and 50 with the peak just past 10. Thus, G/τ ratios of 2–5 to 50 serve as the optimum G/τ window for each domain, based on stability.

Previous work by Kolar *et al.* [20] indicates that the G/τ ratio should lie between 1 and 10 if the modeler is concerned about minimizing mass balance errors and errors in the generation of non-linear constituents. They also showed that as the G/τ ratio increases above 100, oscillations will start to appear in the solutions. Comparing this to the results of the sensitivity analyses above, we can see that the optimum G/τ ratios overlap in the range of 2–10. Thus,

[4] We did also look at sensitive changes by varying G in the original algorithm concurrently with the predictor–corrector algorithm. Shapes of the sensitivity graphs changed, particularly for the constant bathymetry, but general conclusions remain unaltered.

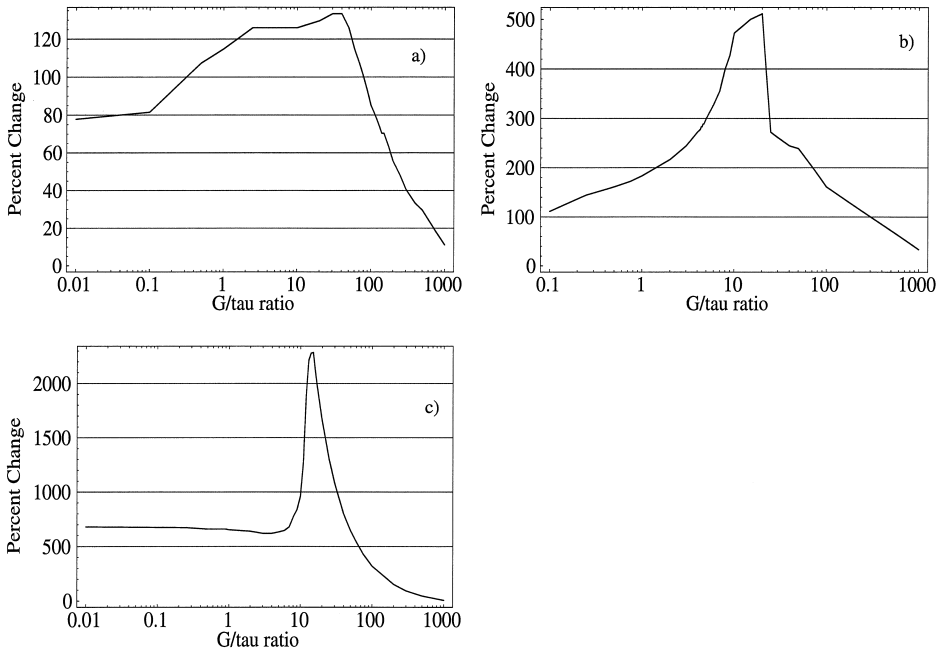

Figure 3. Sensitivity of stability to the G/τ ratio for one-dimensional bathymetries: (a) constant, (b) second-order, (c) east coast (note: G/τ ratio is G/τ ratio.)

if we keep G/τ between 2 and 10, we will be able to see both an increase in stability and a decrease in mass balance errors and errors in the generation of non-linear constituents, yet not allow the generation of spurious modes.

5.6. Temporal accuracy tests

To evaluate accuracy, we compared a solution using a large time step to a 'true solution' of the same problem. For temporal accuracy, the 'true solution was obtained using a very fine time step of one second. Accuracy changes were quantified by analyzing the error, as measured by pointwise convergence, L_2 norm, and L_∞ norm, between the fine and coarse solutions. Three domains utilized in the accuracy testing were the constant, second-order and the east coast bathymetries. Each domain was divided spatially into 51 nodes utilizing constant discretization.

Simulations used the centered scheme for the non-linear terms, where the GWCE non-linear terms were centered at k and NCM non-linear term was centered at $k + 1/2$. Accuracy changes were examined for the original algorithm, predictor–corrector algorithm with one corrector iteration (1st iteration), and predictor–corrector algorithm with two corrector iterations (2nd iteration). For each domain, the L_2 and L_∞ norms were evaluated at 50 discrete times covering two complete tidal cycles and then averaged. Pointwise convergence was evaluated for the last

output recorded at three nodes within the domain: node 3 (near ocean boundary), node 25 (middle) and node 47 (near land boundary). Figure 4(a)–(c) shows results using the L_2 norm for elevation for the three domains.

In all domains, the 2nd iteration provided no improvement to the accuracy, which indicates that global convergence was obtained with only one corrector iteration. For all three domains, results showed that the predictor–corrector results plotted below or near the original results, thus indicating equal or less error. The greatest increase in accuracy coincides with domains where more nodes are located in shallow regions. On the other hand, for domains such as the east coast, where most nodes are located in deep water, there are few gains in accuracy. One explanation for this is that wave propagation in deep waters is a weakly non-linear problem, hence updating non-linear terms is inconsequential. For the constant and second-order problems, the order of accuracy increased from first-order with the original algorithm to nearly second-order with the predictor–corrector algorithm, based on the slope of the L_2 and L_∞ graphs. As for the pointwise convergence test, we determined the same changes in the order of accuracy for the middle node; however, the results for nodes near the ocean or land boundaries are influenced by the boundary conditions and were inconclusive. Accuracy changes for the velocity results provided similar findings.

5.7. Scaling analysis

Scaling analysis is used to estimate the order of magnitude of the terms in a differential equation; they have been proven useful in estimating the relative importance of each term in shallow water models (e.g. Mellor [23]). Basically, the objective is to recast terms of the equation from the differential form to an algebraic form so that its relative magnitude can be estimated from known parameter values. Note that the finite amplitude term was split into two portions (see Equation (4)) due to the treatment of this term in the solution scheme, where the linear portion (first term on r.h.s. of Equation (4)) is already treated implicitly, while the non-linear portion (second term on right-hand side of Equation (4)) is only treated implicitly with the predictor–corrector algorithm

$$\nabla \cdot Hg\nabla\zeta = \nabla \cdot hg\nabla\zeta + \nabla \cdot \zeta g\nabla\zeta \tag{4}$$

Scaling of the non-linear terms is shown in Table V. In this analysis, we are trying to establish if a correlation exists between the scaled value of the non-linear terms and the results from the stability experiments. Scaled values of the non-linear terms were normalized to the time derivative term for each equation in order to make the analysis dimensionless.

Domains used in this analysis were the constant, second-order, and the east coast bathymetries, all with a constant spatial discretization. Parameters for evaluating the scaled terms are shown in Table VI. Note that G and τ values are typical simulation values, while T is the period of one M_2 tide and L_∞ is one-half the wavelength of the M_2 tide. Each domain was divided into 51 nodes; bathymetry values (see Table VI) for the scaling analysis were taken from the third node (near the ocean boundary) and the 47th node (near the land boundary). These two nodes were chosen because we wanted to analyze sensitivity of the scaling results to deep and shallow ocean bathymetries. Elevation and velocity values come from a 14-h

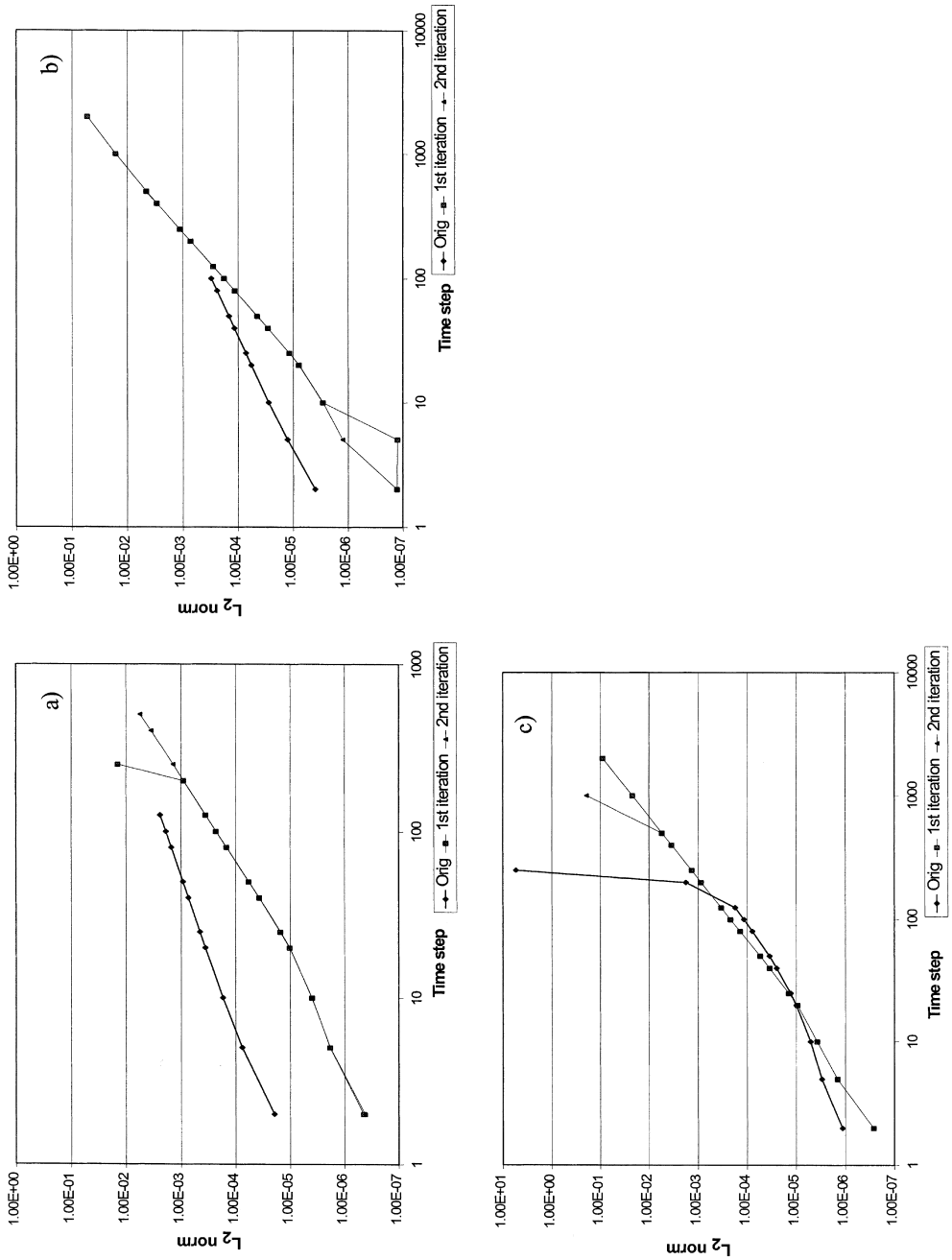

Figure 4. Results of the temporal accuracy tests: (a) constant, (b) second-order, (c) east coast.

Table V. Scaled form of the non-linear terms

Abbreviations	Non-linear term	Scaled form
ag	$\nabla \cdot \{\nabla \cdot (H\mathbf{vv})\}$	$\frac{1}{L}\left(\frac{Huu}{L}\right)$
fg (non-linear portion)	$\nabla \cdot \zeta g \nabla \zeta$	$\frac{1}{L}\left(g\zeta\frac{\zeta}{L}\right)$
fg (linear portion)	$\nabla \cdot hg \nabla \zeta$	$\frac{1}{L}\left(gh\frac{\zeta}{L}\right)$
Gg	$G\nabla \cdot (H\mathbf{v})$	$G\left(\frac{Hu}{L}\right)$
bg	$\tau\nabla \cdot (H\mathbf{v})$	$\tau\left(\frac{Hu}{L}\right)$
am	$\mathbf{v} \cdot \nabla \mathbf{v}$	$\frac{uu}{L}$

(constant bathymetry) or 50-h (second-order and east coast) simulation. Normalized values were then compared to the results of the stability experiments, where each term was evaluated individually (see Table IV). Results from the stability experiments are scaled to the GWCE flux times G term (Gg), since this term is the most influential term in that study.

Figure 5(a)–(c) illustrates the trends, where the bars show results of the scaling analysis and the lines show the results of the stability experiments; the left y-axis is associated with the bars and the right y-axis accompanies the line on each graph. Deeper bathymetries (third node) are the open bars, while the cross-hatched bars are the shallower bathymetries (47th node). Non-linear terms, designated by their appropriate abbreviations, are shown on the x-axis. A positive correlation exists if one or both of the bars follows the same trend as the line.

Table VI. Parameters used in the scaling analysis

Parameter	Bathymetry		
	Constant	Second-order	East coast
h-shallow (ft)	16.4	13.3	279.4
h-deep (ft)	16.4	870.2	16 404.2
u-shallow (ft s^{-1})	0.48	3.5	1.2
u-deep (ft s^{-1})	6.6	0.45	0.25
ζ-shallow (ft)	4.9	6.0	7.8
ζ-deep (ft)	3.4	3.4	3.3
L-shallow (ft)	517 116	465 817	2 509 345
L-deep (ft)	517 116	3 766 372	16 352 643
T (s)	45 000	45 000	45 000
G (s^{-1})	0.001	0.001	0.001
τ (s^{-1})	0.0001	0.0001	0.0001

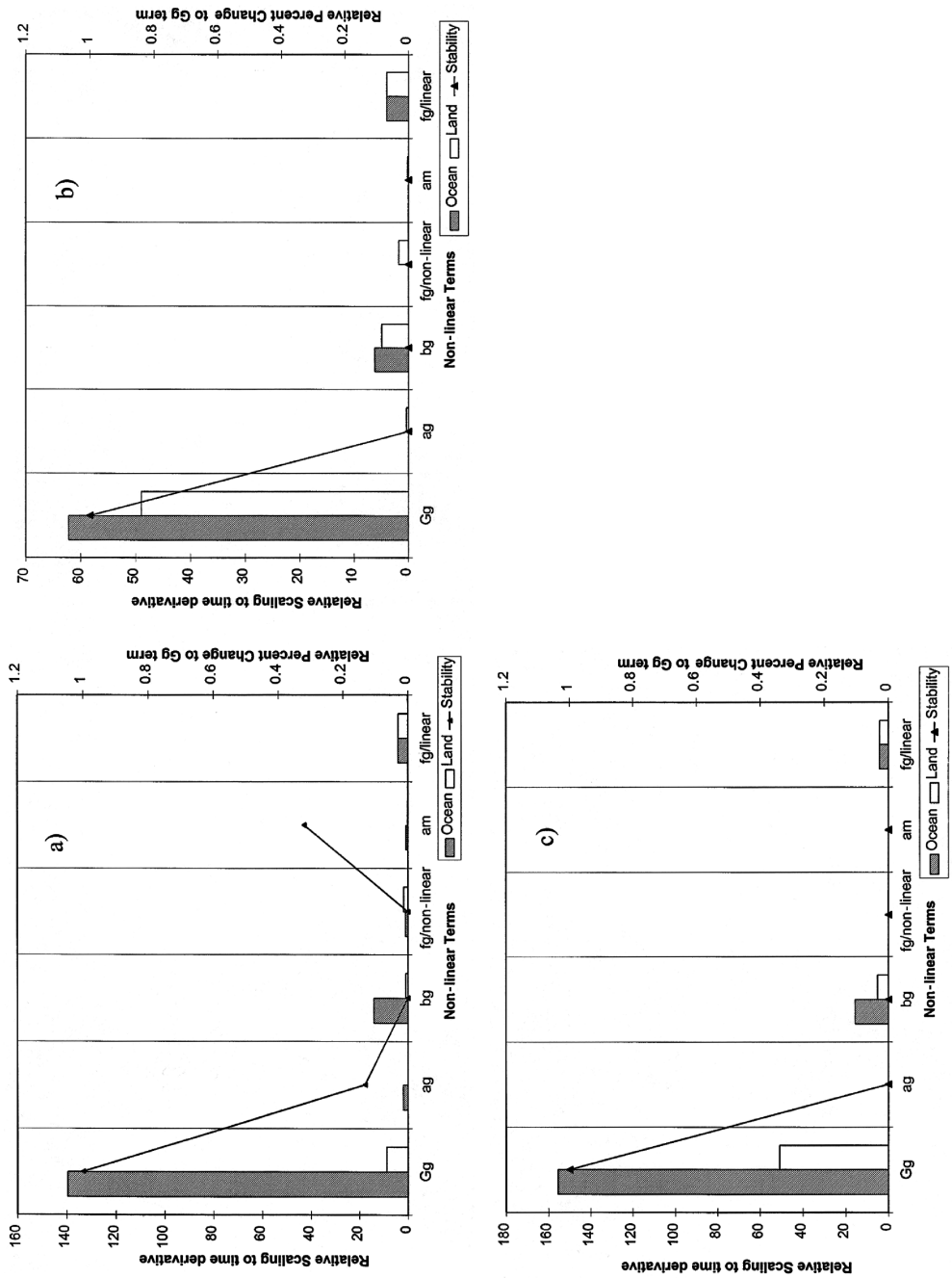

Figure 5. Results of the scaling analysis tests (see Table I for nomenclature): (a) constant, (b) second-order, (c) east coast.

In all the domains analyzed, the GWCE flux times G term (Gg) showed that it was significant in both the scaling results and the stability experiments results, thus implying that there is a positive correlation. We also see a correlation with the second-order and east coast results for the advective terms of the GWCE and NCM equation in that neither is significant. However, for the constant bathymetry, no correlation for the advective terms is seen, i.e., Figure 5(a) shows that both advective terms were significant in the stability experiment results, but only the GWCE advective term (ag) showed a non-trivial scaled value. No correlation exists for the GWCE flux times τ term (bg) and the finite amplitude term (fg) for any of the domains. It is evident that these latter two non-linear terms did not have a significant impact in the stability experiments, but in the scaling analysis, they show some significance, particularly for the deeper portions of the domains.

Focusing now on only the scaling analysis results, we can infer dominant physical processes for each of the domains by looking at the magnitude of each term. In the deeper depths, the advective terms (am and ag) are not significant since the velocity values and gradients are lower due to the heightened water column (see am and ag bars in Figure 5(b)). In the shallow depths, the velocity values and gradients increase due to the shortening of the water column. Thus, in domains where the bathymetry is shallow, the advective terms (am and ag) can be significant, so this term needs to be treated implicitly with the predictor–corrector algorithm (e.g. ag term for constant bathymetry).

Another observation comes from analyzing the behavior of the finite amplitude terms (fg). From the scaling analysis of the second-order bathymetry, we notice that the non-linear portion of this term is significant in the shallow portions of the domains (see Figure 5(b)) because the change in the elevation is larger. Thus in domains where the bathymetry values are predominantly shallow, the non-linear portion of the finite amplitude term is often significant, so it should be treated implicitly when using the predictor–corrector algorithm. As for the linear portion of the finite amplitude term, the scaling analysis shows that it is significant in both deep and shallow bathymetries. Taken together, the results indicate that the finite amplitude term in Equation (2) should always be treated implicitly.

The relative significance of the GWCE flux terms (Gg and bg) depends primarily on the value of τ and its relation to the G-parameter. Only when τ is equal to or greater than the G-parameter will the GWCE flux times τ term (bg) be as significant as the GWCE flux times G term (Gg). In most domains, the G-parameter is chosen to be equal to or greater than the τ-parameter (optimum G/τ between 2 and 10, as recommend by Kolar *et al.* [20] and also indicated by the sensitivity studies in this paper). For the upper end of this range, the GWCE flux times τ term (bg) need not be treated implicitly when using the predictor–corrector algorithm, but the GWCE flux times G term (Gg) must be treated implicitly. On the other hand, if G and τ are of the same magnitude, or if a non-linear parameterization of τ (e.g. Chezy equation) is used wherein its value is not known *a priori*, then both should be treated implicitly.

In summary, the most significant term throughout the scaling analysis has been the GWCE flux times G term (Gg), and it is the only one consistently showing strong positive correlations; all other non-linear terms have a regional impact. These results indicate that the GWCE flux times G term (Gg) should always be treated implicitly. The GWCE advective term (ag) and the NCM advective term (am) should be treated implicitly in the predictor–corrector algorithm for

simulations that have regions of high advective accelerations. The finite amplitude term (fg) should be treated implicitly for both shallow and deep water simulations, and the GWCE flux times τ term (bg) should be treated implicitly when G and τ are the same order of magnitude (or if a non-linear parameterization of τ is used). Thus, codes using this predictor–corrector algorithm should allow the user the option to select which non-linear terms to update in the corrector loop.

6. CONCLUSIONS

The primary objectives of this paper were to examine the use of a predictor–corrector algorithm for one-dimensional simulations and quantify its affect on stability and accuracy. Influence of mesh generating techniques ($\lambda/\Delta x$ versus LTEA) was also examined for the east coast bathymetry. Lastly, a scaling analysis was used to determine if a correlation exists between the relative magnitude of the non-linear terms and the results from the stability experiments.

In general, the predictor–corrector algorithm allows a dramatic increase in the maximum stable time step for all the domains examined. Significant conclusions that we can draw from this study are listed below.

- Only one iteration of the corrector step in the predictor–corrector algorithm is necessary, both in terms of stability and accuracy.
- When evaluating the non-linear terms individually with the predictor–corrector algorithm, there is at least 100 per cent gain in the maximum stable time step for most of the test problems evaluated. For some of the simulations, there is a tenfold increase in the results.
- Stability results show the maximum increase occurs when the non-linear terms were evaluated either four at a time or all five at a time.
- The GWCE flux times G term (Gg) influences stability the most.
- Experiments showed that stability is influenced by the mesh generating technique.
- From the G sensitivity study, it is evident that the G values that produce minimal mass balance errors and errors in the generation of the non-linear constituents coincide with those that produce the maximum stable time step (G/τ between 2–5 and 10).
- Temporal accuracy tests show that the predictor–corrector algorithm reduces absolute error and increases the order of accuracy. In fact, the order of accuracy changes from being first-order with the original algorithm to nearly second-order with the predictor–corrector algorithm for highly non-linear problems.
- From the scaling analysis, we see that the GWCE flux times G (Gg) is the most significant of the non-linear terms in the domains evaluated.
- Also from the scaling analysis, it was evident that the finite amplitude term (fg) is significant in both the shallow and deep parts of the domains; the GWCE flux times τ term (bg) is only significant if the G-parameter is less than or equal to the τ-parameter or if a non-linear parameterization of τ is used.
- Stability improvement and the optimum set of time weights are grid and problem dependent; thus, there needs to be an option that allows the user to treat some or all the

non-linear terms implicitly. Lacking performance testing, we generally recommend that all the GWCE non-linear terms should be centered at k and the NCM non-linear term should be centered at $k+1/2$.

It is apparent from these results that the predictor–corrector algorithm significantly enhances the ability of ADCIRC to perform fast, reliable simulations. Studies with a wide variety of two-dimensional domains is on-going and will be reported in a subsequent article.

ACKNOWLEDGMENTS

We thank the anonymous reviewers for their constructive comments. Financial support for this research was provided in part by the National Science Foundation under the contract ACI-9623592. Any opinions, findings, conclusions or recommendations expressed in this material are those of the authors and do not necessarily reflect those of the National Science Foundation.

APPENDIX A. NOMENCLATURE

$\mathbf{A}$	atmospheric force (L^2/T^2)
c	linear wave celerity
C_r	Courant number, equals $c\Delta t/\Delta x$
C^0	set of continuous functions over Ω whose first derivative is, at most, discontinuous at a finite number of points in Ω
f	Coriolis parameter, equals $2\Omega \sin \phi$
g	gravity $\lvert\mathbf{g}\rvert$ (L/T^2)
G	numerical parameter in the generalized wave continuity equation ($1/T$)
h	bathymetry (L)
H	total fluid depth, equals $h+\zeta(L)$
i	spatial index
k	time-weighting parameter, temporal index
L	length
L	symbol for primitive continuity equation
M	mass
$\mathbf{M}$	symbol for primitive momentum equation, non-conservative form
$\mathbf{M}^C$	symbol for primitive momentum equation, conservative form
p	pressure (M/LT^2)
p_a	atmospheric pressure (M/LT^2)
t	time
T	time period for tidal constituents (T)
$\mathbf{T}$	macroscopic stress tensor (M/LT^2)
u	scalar fluid velocity in one-dimensional problem (L/T)
$\mathbf{v}$	velocity of the fluid (L/T)
W^G	symbol for the generalized wave continuity equation

Greek letters

α	earth elasticity factor
ε	eddy viscosity (L^2/T)
η	Newtonian equilibrium tidal potential
ζ	elevation of water surface above the datum (L)
λ	wavelength
ρ	density (M/V)
τ	bottom friction coefficient ($1/T$)
Ω	angular velocity of the earth ($1/T$)

Special symbols and operators

∇	nabla (grad) operator ($1/L$)
$\nabla\cdot$	divergence operator ($1/L$)
$\partial/\partial t$	partial derivative ($1/T$)

REFERENCES

1. Kolar RL, Gray WG, Westerink JJ, Luettich RA. Shallow water modeling in spherical coordinates: equation formulation, numerical implementation and application. *Journal of Hydraulic Research* 1994; **32**(1): 3–24.
2. Lynch DR, Gray WG. A wave equation model for finite element tidal computations. *Computers and Fluids* 1979; **7**(3): 207–228.
3. Kinnmark IPE. The shallow water wave equations: formulations, analysis and application. In *Lecture Notes in Engineering*, vol. 15, Brebbia CA, Orszag SA (eds). Springer-Verlag: Berlin, 1986; 187.
4. Luettich RA, Westerink JJ, Scheffner NW. ADCIRC: an advanced three-dimensional circulation model for shelves, coasts and estuaries. Report 1: theory and methodology of ADCIRC-2DDI and ADCIRC-3DL. Technical Report DRP-92-6, Department of the Army, USACE, Washington, DC, 1992.
5. Westerink JJ, Luettich RA, Blain CA, Scheffner NW. ADCIRC: an advanced three-dimensional circulation model for shelves, coasts and estuaries. Report 2: Users Manual for ADCIRC-2DDI, Department of the Army, USACE, Washington, DC, 1994.
6. Kolar RL, Looper JP, Westerink JJ, Gray WG. An improved time marching algorithm for GWC shallow water models. In *CMWR XII: Computational Methods in Surface Flow and Transport Problems*, vol. 2, Burganos VNI, Karatzas GP, Payatakes AC, Brebbia CA, Gray WG, Pinder GF (eds). Computational Mechanics Publications: Southampton, 1998; 379–385.
7. Lee JK, Froehlich DC. Review of Literature on the Finite-Element Solution of the Equations of Two-dimensional Surface-Water Flow in the Horizontal Plane. US Geological Survey Circular 1009, USDOI, Denver, CO, 1986.
8. Gray WG, Lynch DR. Time-stepping schemes for finite element tidal model computations. *Advances in Water Resources* 1977; **1**(2): 83–95.
9. Kinnmark IPE, Gray WG. An implicit wave equation model for the shallow water equations. *Advances in Water Resources* 1984; **7**: 168–171.
10. Blain CA. The influence of domain size and grid structure on the response characteristics of a hurricane storm surge model. PhD dissertation, Notre Dame, 1994.
11. Hagen SC, Westerink JJ, Kolar RL. One-dimensional finite element grids based on a localized truncation error analysis. *International Journal for Numerical Methods in Fluids* 2000; **32**(2): 241–261.
12. Luettich RA, Westerink JJ. Implementation and testing of elemental flooding and drying in the ADCIRC hydrodynamic model. Final Report, 8/95, Contract # DACW39-94-N-5689, 1995.
13. Kolar RL, Gray WG, Westerink JJ. Boundary conditions in shallow waster models—an alternative implementation for finite element codes. *International Journal for Numerical Methods in Fluids* 1996; **22**(7): 603–618.
14. Lynch DR, Holboke MJ. Normal flow boundary conditions in 3D circulation models. *International Journal for Numerical Methods in Fluids* 1997; **25**(10): 1185–1205.
15. Lynch DR, Werner FE, Greenberg DA, Loder JW. Diagnostic model for baroclinic and wind-driven circulation in shallow seas. *Continental Shelf Research* 1992; **12**(1): 37–64.
16. Lynch DR. Three-dimensional Diagnostic Model for Baroclinic, Wind-driven and Tidal Circulation in Shallow Seas—FUNDY4 User's Manual. Numerical Methods Laboratory Report, 1990.

17. Muccino JC, Gray WG, Foreman MGG. Calculation of vertical velocity in three dimensional shallow water equation, finite element models. *International Journal for Numerical Methods in Fluids* 1997; **25**(7): 779–802.
18. Chippada S, Dawson CN, Wheeler MF, Martinez ML. Parallel computing for finite element models of surface water flow. In *CMWR XI: Computational Methods in Surface Flow and Transport Problems*, vol. 2, Aldama AA, Aparicio J, Brebbia CA, Gray WG, Herrera I, Pinder GF (eds). Computational Mechanics: Southampton, 1996; 63–70.
19. Kashiyama K, Saito K, Yoshikawa S. Massively parallel finite element method for large scale computation of storm surge. In *CMWR XI: Computational Methods in Surface Flow and Transport Problems*, vol. 2, Aldama AA, Aparicio J, Brebbia CA, Gray WG, Herrera I, Pinder GF (eds). Computational Mechanics: Southampton, 1996; 79–86.
20. Kolar RL, Westerink JJ, Cantekin ME, Blain CA. Aspects of non-linear simulations using shallow-water models based on the wave continuity equation. *Computers and Fluids* 1994; **23**: 523–528.
21. Lynch DR, Werner FE. Three-dimensional hydrodynamics on finite elements. Part II: non-linear time-stepping model. *International Journal for Numerical Methods in Fluids* 1991; **12**: 507–533.
22. Hagen S. Finite element grids based on a localized truncation error analysis. PhD dissertation, Department of Civil Engineering, Notre Dame, 1996.
23. Mellor GL. *Introduction to Physical Oceanography*. Springer-Verlag: New York, 1996; 260.

